Journal of Materials Chemistry A

Accepted Manuscript

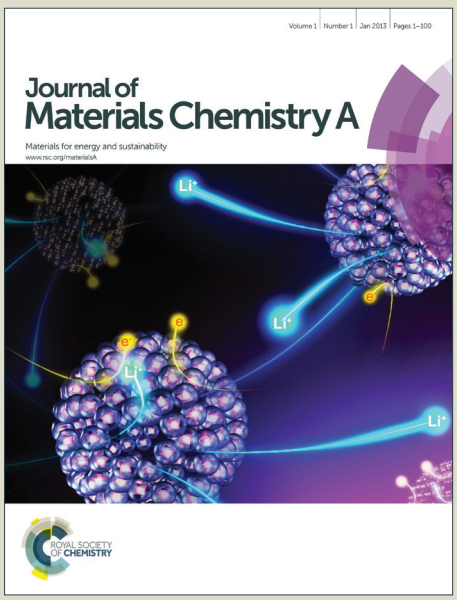

ROYAL SOCIETY OF CHEMISTRY

www.rsc.org/materialsA

Journal of Materials Chemistry A

Dynamic Article Links ►

Cite this: DOI: 10.1039/c0xx00000x

www.rsc.org/xxxxxx

Communication

Facile and Economical Mass Production of Graphene Dispersions and Flakes

Min Mao,[a] Shuzhen Chen,[a] Ping He,[b] Hailin Zhang,[a] Hongtao Liu*[a c]

Received (in XXX, XXX) Xth XXXXXXXXX 20XX, Accepted Xth XXXXXXXXX 20XX

DOI: 10.1039/b000000x

Here we illustrate a facile and economical strategy for the bulk production of aqueous graphene dispersions via a simple ball milling process assisted with little non-ionic industrial surfactant. Moreover, this surfactant is readily removed using ethanol to acquire high-quality graphene flakes. The fabricated graphene electrode shows excellent high-rate charge-discharge performance suitable for supercapacitor application.

Due to its fascinating properties such as intrinsically superior electrical conductivity, high specific surface area, excellent mechanical strength, and remarkable thermal conductivity, graphene, a sp^2-bonded one-atomic thick fully conjugated quasi-two-dimensional hexagonal carbon molecule lattice, has garnered ever increasing attentions from both academia and industry during recent years[1]. To accelerate its various potential applications, it is significantly important to search for facile routes to fabricate graphene in bulk production at low cost since mechanical cleavage of graphite originally leading to the discovery of graphene sheets in 2004[2] is time-consuming and low-yield. To date, various other preparation processes, including direct exfoliation in solvents[3], unzipping of carbon nanotubes[4], electrochemical strategy[5] and organic synthetic protocols[6], have been developed. While there are only two methods potentially capable of quantity production of few-layer graphene (FLG) flakes. One is the most commonly-used strategy of chemical oxidation-reduction of pristine graphite[7] to obtain reduced graphene oxide flakes in large-scale production. However, this strategy suffers many drawbacks, such as fussy and time-consuming preparation process, tedious impurities removal, and heavy defects in the product caused by harsh oxidants and corrosive acids. The other popular method for scalable production of graphene is based on epitaxial growth on silicon carbide or metal substrates using chemical vapor deposition (CVD)[8, 9]. Although the produced FLG films are with low levels of defects and impurities, the fabrication cost is very high due to the expensive substrate and apparatus. Besides, the process is very complex and generally involves transfer of graphene from substrate.

Recently, ball milling technology has been tasted to fabricate graphene materials in terms of simple operation and mass production. Liming Dai's group and Jong-Beom Baek's group have efficiently prepared edge-selectively functionalized graphene nanoplatelets (EFGnPs), such as hydroxyl-functionalized graphene[10], edge-carboxylated graphene nanosheets[11] and hydrogen-, carboxylic acid-, sulfonic acid-, and carboxylic acid/sulfonic acid- functionalized GnPs[12], simply by ball milling graphite in the presence of potassium hydroxide, dry ice, and hydrogen, carbon dioxide, sulfur trioxide, or carbon dioxide/sulfur trioxide mixture, respectively. Chen et al.[13] acquired graphene flakes in N,N-dimethylformamide (DMF) medium via a shear-force-dominated ball milling method, in which the DMF-graphene interactions are supposed to be stronger than the Van der Waals-like coupling forces between graphite layers. Peukert et al.[14] mechanically peeled graphene off in assistant with ionic surfactant sodium dodecyl sulfate (SDS) by stirred media mills, wherein the SDS surfactant can stabilize graphene flakes against agglomeration and restacking. However, DMF is a toxic solvent with high boiling point 153℃, thus hard to remove. The ionic surfactant is susceptible to inorganic salt, acid, or alkaline, lacking of stability. Therefore, it is desirable in search of safer solvents and more reliable surfactants for ball-milling production of high-quality graphene materials.

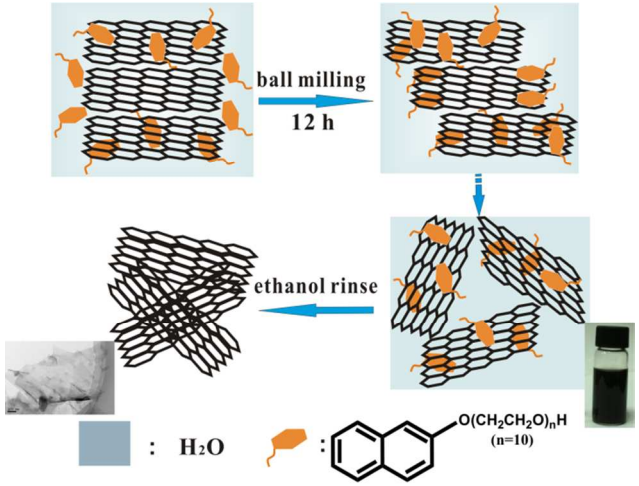

Figure 1 Illustration of production of aqueous graphene dispersions with naphthol polyoxyethylene ether (NPE).

In this communication, we demonstrate an efficient ball-milling synthesis of FLG flakes, wherein, an industrially non-ionic surfactant, naphthol polyoxyethylene ether (NPE) is employed as both assistant detacher and stabilizer. Fundamentally, our strategy offers the following four significant advantages. Firstly, the method is mild and environment-friendly (no any harsh and toxic reactants); Secondly, it is simple (based on ball milling) and productive (readily gram-scale in the lab); Thirdly, the used non-ionic surfactant is cheap but very effective to assist exfoliation and prevent graphene restacking; Fourth, the high-concentration (0.5-1.2 mg/ml) dispersions are conveniently transformed into FLG flakes only by ethanol rinse.

Figure 1 illustrated the production of aqueous graphene dispersions. NPE, composed of a big π-electron aromatic ring and a long alkoxy tail, shows evident amphiphilic characteristics. Under continuously ball-milling shearing force, the graphite layers tend to separate, and are promptly carpeted with NPE in terms of the strong π-π interaction between the naphthol ring and the graphene ring. The detached graphene flakes are therefore stabilized without restacking. The activated energy for exfoliation of graphite is supplied by ball-milling shearing force. The NPE-covered graphene flakes are well dispersed in water due to the protruding hydrophilic alkoxy chain of NPE.

The overall potential energy of two parallel, 2D sheets coated with surfactants can be written as

$$V_T \approx \frac{\alpha A \kappa T L}{s^3} e^{-\pi D/L} - \frac{A\pi\rho^2 C}{2D^4} \qquad (1)$$

The $-A\pi\rho^2C/2D^4$ part is the attractive vdw (Van der Waals' force) potential energy[15, 16] between graphene layers, where A is the graphene surface area, ρ is the number of active sites per unit area on the surface, D is the layer separation, and C is the constant. The $\alpha A\kappa TLe^{-\pi D/L}s^{-3}$ part is the steric repulsive potential[15, 17] between the protruding hydrophilic tails, where α is a constant, L is the length of the protruding group and s is the mean distance between attachment points. As shown in Figure S1, the hydrophobic naphthol part tightly attaches on graphene sheet via π - π interaction, inhibiting the NPE molecules detach from the sheet surfaces and exchange with those in the bulk solution, while the hydrophilic tail of the non-ionic surfactant interacts very strong with water molecules via hydrogen bond, extending into bulk water in meander type. Thus once two surfactant-coated graphene sheets approach each other, the protruding hydrophilic tails begin to interact, resulting in a steric repulsion between the flakes. A small value (-21.4 mV) for zeta potential (Figure S2) also implies the highly dispersed graphene solution is more dependent on the steric repulsion of the surfactants than the electrostatic repulsion of the molecule dipole. We can calculate V_T/A (overall potential energy for unit area) for surfactant-stabilized graphene dispersion as a function of sheet separation, D.

$$\frac{V_T}{A} \approx \frac{\alpha\kappa TL}{s^3} e^{-\pi D/L} - \frac{\pi\rho^2 C}{2D^4} \qquad (2)$$

When $\frac{d\frac{V_T}{A}}{dD} = -\frac{\pi\alpha\kappa T}{s^3} e^{-\pi D/L} + \frac{2\pi\rho^2 C}{D^5} = 0$,

one can get a local maximum point (D_0, $V_{T,\,max}$). It is the presence of the potential barrier, $V_{T,\,max}$, which opposes aggregation and results in the stabilization of surfactant-coated graphene sheets. The exfoliated graphite/NPE flakes are well dispersed in water but not in ethanol (Shown in Figure S3). It should be noted that the color of graphite/NPE solution in ethanol is slight yellow, indicating that ethanol selectively dissolves the surfactant, NPE.

When the UV-vis absorption spectrum[18] of graphite/NPE in water is compared with that of ethanol solution (shown in Figure 2), the graphite/NPE in water shows a wide range absorption of graphene (375–700 nm) with an absorption peak at 330 nm corresponding to the absorption of naphthol part slightly left shift than that of others, whereas the graphite/NPE in ethanol does not show the wide absorption of graphene, indicating that graphite is not exfoliated in ethanol. The poor exfoliation and dispersibility of graphene in ethanol is presumably because both naphthol and polyoxyethylene ether are very soluble in ethanol, while water cannot dissolve naphthol which allows the naphthol part to interact with the graphene surface by π-π interaction. Therefore, ethanol is not a proper solvent for exfoliation and dispersion of graphite, but it would be rather a good lotion for washing out NPE physically absorbed on the graphene surface.

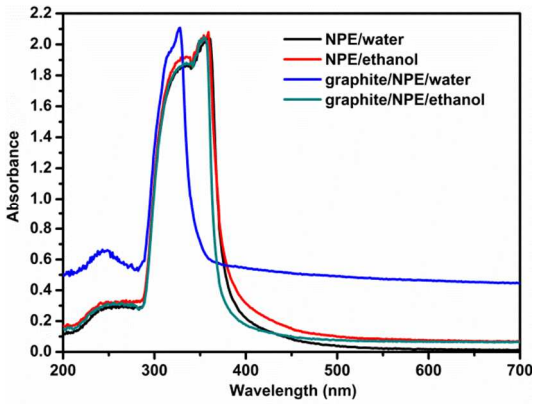

Figure 2 UV-vis absorption spectra of NPE/ethanol (solid red) and graphite/NPE/ethanol (solid green), NPE/water (solid black), and graphite/NPE/water (solid blue).

To probe the quality of the as-obtained graphene surface, we have carried out Fourier transform infrared spectroscopy (FT-IR) study. As shown in Figure S4, the FT-IR spectrum of washed graphene shows a characteristic peak of graphene at ~1600 cm^{-1}, but does not show any characteristic peaks of oxygen-containing functional group[19]. Importantly, FT-IR spectra clearly show the progressive removal of the NPE by ethanol. As as-obtained graphene is washed with ethanol through centrifugation at 13000 rpm, NPE are significantly reduced or entirely removed.

The XPS spectroscopy[10] further confirms the composition of the FLG surface. As shown in Figure 3a, there only exist C peak and O peak in the XPS survey spectrum, and the measured atomic ratio is C:O=19:1. The high-resolution C1s spectrum (Figure 3b) reveals these small quantities of oxygenated groups on the FLG surface are C-O and C-O-C groups.

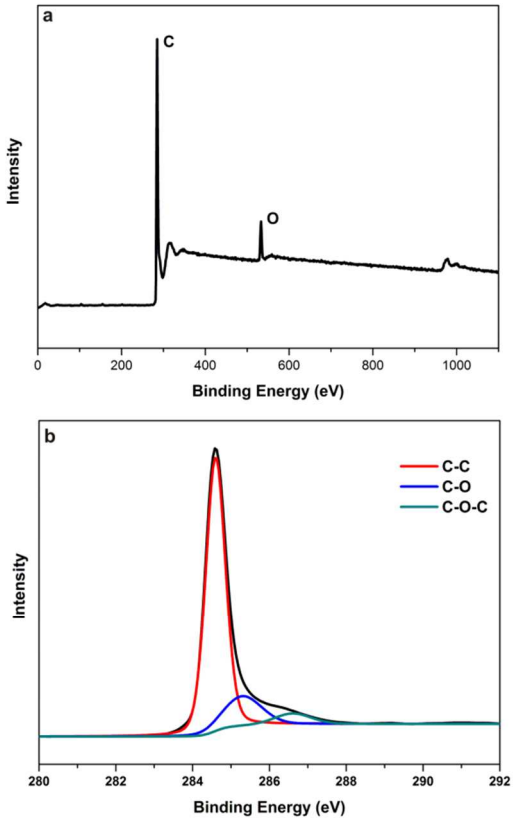

Figure 3 XPS survey spectrum (a) and high-resolution XPS C1s spectrum of of the resultant washed graphene film.

Figure 4(a) shows a representative TEM image of a collection of graphenes and additional TEM images of FLG flakes are available in Figure S5, which show the sheet-like nature of the material. It is found that graphene sheets have a size of several hundred nanometers and some are stacked together. High resolution TEM analysis of the graphene edges (see Figure 4(c), Figure S6) reveals that the majority of the graphene sheets are made of below 10 layers, in line with the AFM result (Figure S7), with a lattice spacing of 0.35 nm. No other carbon phases such as amorphous carbon or fullerene etc. are found at the edges. The corresponding selected electron diffraction pattern of single sheets (Figure 4(d)) has a typical six-fold symmetry, confirming that the graphene sheet is of high-quality single crystal nature. Figure 4(b) is an overlap with a 30° rotation of two hexagons corresponding to double-layer graphene sheets. The hexagonal patterns of the electron diffraction indicate the sp^2 carbon frameworks with low defects and the grapheme sheets exhibit good crystallinity with the structure consistent with graphene. Shown in Figure 4(e) is a HRTEM image of a graphene monolayer, and the Figure 4(f) depicts a fast Fourier transform (FFT) of this image. This is equivalent to an electron diffraction pattern. The [1100] spots can clearly be seen. However, the [2110] spots are too faint to see. This intensity difference is the fingerprint of monolayer graphene[16, 20]. Also the better symmetric 2D band with left shift peak (2700 cm^{-1}) in Raman spectra (see Figure S9) for FLG identifies the successful fabrication of few-layer graphene composed of less than five graphene layers[21, 22].

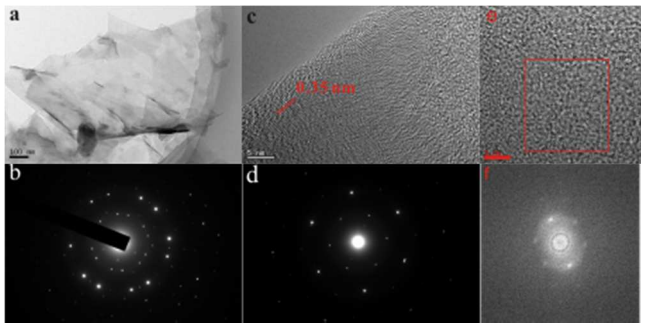

Figure 4 TEM (a) and HRTEM (c, e) of FLG flakes (b, d), electron diffraction patterns (b, d) of graphene sheets and a fast Fourier transform (FFT)(f) of image Figure 3(e).

The electrical characteristics of the graphene film (see Figure S8) hold the key for their future applications. As expected, the unwashed film has a relatively high sheet resistance of 7300 ohm per square, due to the existence of NPE attaching to graphene surface via π - π interaction, whereas the sheet resistance of the graphene film washed with ethanol was as low as 300 ohm per square. The measured resistance data are consistent with the UV-vis absorption and FT-IR results demonstrated above. These demonstrate once again that ethanol is capable of removing almost all NPE from graphene film or solution.

Raman spectroscopy provides a non-destructive method for characterizing graphene. The carbon defects were further confirmed by the Raman spectra at an excitation laser of 532 nm, in which the D peak (~1350 cm^{-1}) implies the disorder of the edge carbons whereas the G band (1580 cm^{-1}) is related to the ordered in-plane sp^2 carbon atoms. Therefore, the intensity ratio (I_D/I_G) is generally accepted to represent the defective carbon fraction. As shown in Figure S9, a slightly greater value I_D/I_G of the washed grapheme film compared with pristine graphite powder indicates an increase in the number of smaller sp^2 domains, and this feature is dominated by edge effects as the Raman excitation beam spot size of ~2 μm is larger than that of the flakes (see Figure 4(a)) in the suction film. However, the relatively small I_D/I_G value and pretty low electrical resistivity observed for the film coupled with the FT-IR result (see Figure S4) strongly suggest that the film we are fabricating is composed of flakes with low defect content. This indicates mechanical ball milling can harvest higher quality FLG flakes than sonicated exfoliation since shear forces are more efficient to detach graphene from graphite sheets.

The high surface-to-volume ratio of carbon nanomaterials such as nanotubes and graphene generally exhibit high specific charge storage. The capacitance behavior of the FLG flakes was also characterized. The fabricated graphene electrode shows nearly symmetrical rectangular shapes at various scan rates (Figure S10), and a small faradic wave is caused by the surface oxygenated groups. The capacitance of the graphene electrode can be estimated by galvanostatic charge-discharge measurement. A high-rate specific capacitance of 96 F/g at 10 A/g is obtained, and within 10,000 cycles the graphene electrode can retain over 98% of the initial capacitance (Figure S11).

Conclusions

In summary, we have demonstrated a facile and economical

strategy for the bulk production of aqueous graphene dispersions with the aid of the non-ionic surfactant, NPE. During the whole synthetic processes, the employed NPE non-ionic surfactant plays key but irreplaceable roles in both detaching pristine graphite powder and preventing graphene restacking. More importantly, this surfactant is readily removed using ethanol to acquire high-quality graphene flakes. The as-fabricated graphene electrode shows excellent performance potentially for supercapacitor application.

The financial support from the NNSF of China (no.20976189), the Fundamental Research Funds for the Central Universities (no.2011JQ024), and the Open-End Fund for the Valuable and Precision Instruments of Central South University (no.CSUZC2013005) is gratefully acknowledged.

Notes and references

1. D. R. Dreyer, R. S. Ruoff and C. W. Bielawski, *Angew. Chem. Int. Ed.*, 2010, **49**, 9336-9344.

2. K. S. Novoselov, A. K. Geim, S. V. Morozov, D. Jiang, Y. Zhang, S. V. Dubonos, I. V. Grigorieva and A. A. Firsov, *Science*, 2004, **306**, 666-669.

3. Y. Hernandez, V. Nicolosi, M. Lotya, F. M. Blighe, Z. Y. Sun, S. De, I. T. McGovern, B. Holland, M. Byrne, Y. K. Gun'ko, J. J. Boland, P. Niraj, G. Duesberg, S. Krishnamurthy, R. Goodhue, J. Hutchison, V. Scardaci, A. C. Ferrari and J. N. Coleman, *Nat. Nanotechnol.*, 2008, **3**, 563-568.

4. D. V. Kosynkin, A. L. Higginbotham, A. Sinitskii, J. R. Lomeda, A. Dimiev, B. K. Price and J. M. Tour, *Nature*, 2009, **458**, 872-876.

5. M. Mao, M. M. Wang, J. Y. Hu, G. Lei, S. Z. Chen and H. T. Liu, *Chem. Commun.*, 2013, **49**, 5301-5303.

6. P. Kissel, R. Erni, W. B. Schweizer, M. D. Rossell, B. T. King, T. Bauer, S. Gotzinger, A. D. Schluter and J. Sakamoto, *Nat. Chem.*, 2012, **4**, 287-291.

7. S. Park and R. S. Ruoff, *Nat. Nanotechnol.*, 2009, **4**, 217-224.

8. S. Grandthyll, S. Gsell, M. Weinl, M. Schreck, S. Hufner and F. Muller, *J. Phys-Condens. Mat.*, 2012, **24**, 314204.

9. V. O. Ozcelik, S. Cahangirov and S. Ciraci, *Phys. Rev. B*, 2012, **85**, 235456.

10. L. Yan, M. M. Lin, C. Zeng, Z. Chen, S. Zhang, X. M. Zhao, A. G. Wu, Y. P. Wang, L. M. Dai, J. Qu, M. M. Guo and Y. Liu, *J. Mate.r Chem.*, 2012, **22**, 8367-8371.

11. I. Y. Jeon, Y. R. Shin, G. J. Sohn, H. J. Choi, S. Y. Bae, J. Mahmood, S. M. Jung, J. M. Seo, M. J. Kim, D. W. Chang, L. M. Dai and J. B. Baek, *PNAS*, 2012, **109**, 5588-5593.

12. I. Y. Jeon, H. J. Choi, S. M. Jung, J. M. Seo, M. J. Kim, L. M. Dai and J. B. Baek, *J. Am. Chem. Soc.*, 2013, **135**, 1386-1393.

13. W. F. Zhao, M. Fang, F. R. Wu, H. Wu, L. W. Wang and G. H. Chen, *J. Mater. Chem.*, 2010, **20**, 5817-5819.

14. C. Knieke, A. Berger, M. Voigt, R. N. K. Taylor, J. Rohrl and W. Peukert, *Carbon*, 2010, **48**, 3196-3204.

15. Israelachvili, J. Intermolecular and Surface Forces. Academic Press: New York, 1991.

16. M. Lotya, Y. Hernandez, P. J. King, R. J. Smith, V. Nicolosi, L. S. Karlsson, F. M. Blighe, S. De, Z. M. Wang, I. T. McGovern, G. S. Duesberg and J. N. Coleman, *J. Am. Chem. Soc.*, 2009, **131**, 3611-3620.

17. R. J. Smith, M. Lotya and J. N. Coleman, *New J Phys*, 2010, **12**,125008.

18. M. S. Kang, K. T. Kim, J. U. Lee and W. H. Jo, *J. Mater. Chem. C*, 2013, **1**, 1870-1875.

19. A. Bagri, C. Mattevi, M. Acik, Y. J. Chabal, M. Chhowalla and V. B. Shenoy, *Nat. Chem.*, 2010, **2**, 581-587.

20. J. C. Meyer, A. K. Geim, M. I. Katsnelson, K. S. Novoselov, T. J. Booth and S. Roth, *Nature*, 2007, **446**, 60-63.

21. A. C. Ferrari, J. C. Meyer, V. Scardaci, C. Casiraghi, M. Lazzeri, F. Mauri, S. Piscanec, D. Jiang, K. S. Novoselov, S. Roth and A. K. Geim, *Phy.s Rev. Lett.*, 2006, **97**,187401.

22. D. Graf, F. Molitor, K. Ensslin, C. Stampfer, A. Jungen, C. Hierold and L. Wirtz, *Nano. Lett.*, 2007, **7**, 238-242.